

1 Trait paranoia shapes inter-subject synchrony in brain activity during an ambiguous  
2 social narrative

3

4 Emily S. Finn\*<sup>1</sup>, Philip R. Corlett<sup>2</sup>, Gang Chen<sup>3</sup>, Peter A. Bandettini<sup>1</sup>, R. Todd Constable<sup>4</sup>

5

6 <sup>1</sup>Section on Functional Imaging Methods, Laboratory of Brain and Cognition, National Institute  
7 of Mental Health; Bethesda, Md.

8 <sup>2</sup>Department of Psychiatry, Yale School of Medicine; New Haven, Conn.

9 <sup>3</sup>Scientific and Statistical Computing Core, National Institute of Mental Health; Bethesda, Md.

10 <sup>4</sup>Department of Radiology and Biomedical Imaging, Yale School of Medicine, New Haven, Conn.

11

12 \*Corresponding author: [emily.finn@nih.gov](mailto:emily.finn@nih.gov)

13

14 **ABSTRACT**

15 Individuals often interpret the same event in different ways. How do personality traits modulate  
16 brain activity evoked by a complex stimulus? Here we report results from a naturalistic paradigm  
17 designed to draw out both neural and behavioral variation along a specific dimension of interest,  
18 namely paranoia. Participants listen to a narrative during functional MRI describing an ambiguous  
19 social scenario, written such that some individuals would find it highly suspicious, while others  
20 less so. Using inter-subject correlation analysis, we identify several brain areas that are  
21 differentially synchronized during listening between participants with high- and low trait-level  
22 paranoia, including theory-of-mind regions. Follow-up analyses indicate that these regions are  
23 more active to mentalizing events in high-paranoia individuals. Analyzing participants' speech as  
24 they freely recall the narrative reveals semantic and syntactic features that also scale with paranoia.  
25 Results indicate that a personality trait can act as an intrinsic 'prime', yielding different neural and  
26 behavioral responses to the same stimulus across individuals.

27           That different individuals may see the same event in different ways is a truism of human  
28 nature. Examples are found at many scales, from low-level perceptual judgments to interpretations  
29 of complex, extended scenarios. This latter phenomenon is known as the “Rashomon effect”<sup>1</sup> after  
30 a 1950 Japanese film in which four eyewitnesses give contradictory accounts of a crime and its  
31 aftermath, raising the point that for multifaceted, emotionally charged events, there may be no  
32 single version of the truth.

33           What accounts for these individual differences in interpretation? Assuming everyone has  
34 access to the same perceptual information, personality traits may bias different individuals toward  
35 one interpretation or another. Paranoia is one such trait, in that individuals with strong paranoid  
36 tendencies may be more likely to assign a nefarious interpretation to otherwise neutral events<sup>2</sup>.  
37 While paranoia in its extreme is a hallmark symptom of schizophrenia and other psychoses, trait-  
38 level paranoia exists as a continuum rather than a dichotomy<sup>3,4</sup>: on a behavioral level, up to 30  
39 percent of people report experiencing certain types of paranoid thoughts (e.g., ‘I need to be on my  
40 guard against others’) on a regular basis<sup>5</sup> and trait paranoia in the population follows an  
41 exponential, rather than bimodal, distribution<sup>6</sup>.

42           Few neuroimaging studies have investigated paranoia as a continuum; the majority simply  
43 contrast healthy controls and patients suffering from clinical delusions. However, a handful of  
44 reports from subclinical populations describe patterns of brain activity that scale parametrically  
45 with tendency toward paranoid or delusional ideation. For example, it has been reported that  
46 higher-paranoia individuals show less activity in the medial temporal lobe during memory retrieval  
47 and less activity in the cerebellum during sentence completion<sup>7</sup>, less activity in temporal regions  
48 during social reflection<sup>8</sup> and auditory oddball detection<sup>9</sup>, but higher activity in the insula and  
49 medial prefrontal cortex during self-referential processing<sup>10</sup> and differential patterns of activity in  
50 these regions as well as the amygdala while viewing emotional pictures<sup>11</sup>.

51           Such highly controlled paradigms enable precise inferences about evoked brain activity,  
52 but potentially at the expense of real-world validity. For example, brain response to social threat  
53 is often assessed with decontextualized static photographs of unfamiliar faces presented rapidly in  
54 series<sup>12</sup>. Compare this to threat detection in the real world, which involves perceiving and  
55 interacting with both familiar and unfamiliar faces in a rich, dynamic social context. Paranoid  
56 thoughts that eventually reach clinical significance usually have a slow, insidious onset, involving  
57 complex interplay between a person’s intrinsic tendencies and his or her experiences in the world.

58 In studying paranoia and other trait-level individual differences, then, is important to complement  
59 highly controlled paradigms with more naturalistic stimuli.

60 Narrative is an attractive paradigm for several reasons. First, narrative is an ecologically  
61 valid way to study belief formation in action. Theories of fiction posit that readers model narratives  
62 in a Bayesian framework in much the same way as real-world information<sup>13</sup>, and story  
63 comprehension and theory-of-mind processes share overlapping neural resources<sup>14</sup>. Second, a  
64 standardized narrative stimulus provides identical input, so any variation in interpretation reflects  
65 individuals' intrinsic biases in how they assign salience, learn and form beliefs. Third, from a  
66 neuroimaging perspective, narrative listening is a continuous, engaging task that involves much of  
67 the brain<sup>15</sup> and yields data lending itself to innovative, data-driven analyses such as inter-subject  
68 correlation<sup>16,17</sup>.

69 Previous work has shown that experimenters can manipulate patterns of brain activity  
70 during naturalistic stimuli by explicitly instructing participants to focus on different aspects of the  
71 stimulus. For example, Cooper et al. reported that activity patterns in temporal and frontal regions  
72 varied according to whether listeners were told to pay attention to action-, space- or time-related  
73 features of short stories<sup>18</sup>. Lahnakoski et al. showed participants the same movie twice, asking  
74 them to adopt different perspectives each time, and found differences in neural synchrony  
75 depending on which perspective had been taken<sup>19</sup>. Most recently, Yeshurun et al. presented  
76 participants with a highly ambiguous story with at least two plausible—but very different—  
77 interpretations, and used explicit primes to bias each participant toward one interpretation or the  
78 other. Responses in higher-order brain areas, including default mode, were more similar among  
79 participants who had received the same prime, indicating that shared beliefs have a powerful effect  
80 on how individuals perceive an identical stimulus<sup>20</sup>. However, while informative, these studies  
81 have all relied on an explicit prime or instruction; they cannot explain why individuals often  
82 spontaneously arrive at different interpretations of the same stimulus.

83 In this work, we use participants' intrinsic personality traits as an implicit prime, relating  
84 individual differences in trait paranoia to brain activity during a naturalistic task in which  
85 participants are faced with complex, ambiguous social circumstances. Using an original narrative,  
86 we show that while much of the brain is synchronized across all participants during story listening,  
87 stratifying participants based on trait paranoia reveals an additional set of regions with stereotyped  
88 activity only among high-paranoia individuals; many of these are regions involved in theory-of-

89 mind and mentalizing. An encoding model of the task suggests that these regions, including the  
90 temporal pole and medial prefrontal cortex, are particularly sensitive to “mentalizing events” when  
91 the main character is experiencing an ambiguous social interaction or explicitly reasoning about  
92 other characters’ intentions. Finally, we measure participants’ behavioral reactions to the narrative  
93 by analyzing their speech as they freely recall the story, and identify semantic and syntactic  
94 features that vary dimensionally with trait paranoia. Together, results indicate that a personality  
95 trait, in this case paranoia, can modulate both neural and behavioral responses to a single stimulus  
96 across individuals.

97

98

## 99 **RESULTS**

100

### 101 **Behavioral data and task performance**

102 We created a fictional narrative to serve as the stimulus for this study. The narrative  
103 described a main character faced with a complex social scenario that was deliberately ambiguous  
104 with respect to the intentions of certain characters; it was designed such that different individuals  
105 would interpret the events as more nefarious and others as less so. A synopsis of the story is given  
106 in Supplementary Note 1.

107 Twenty-two healthy participants listened to a pre-recorded audio version of the narrative  
108 (total duration = 21:50 min:sec, divided into three parts) during fMRI scanning. Following each  
109 of the three parts, participants answered three challenging multiple-choice comprehension  
110 questions to ensure they had been paying attention. Performance was very accurate (15 of the 22  
111 subjects answered 9/9 [100%] questions correctly, while five answered 8/9 [89%] correctly and  
112 two answered 7/9 [78%] correctly). Self-report data indicated that subjects generally found the  
113 narrative engaging and easy to pay attention to (engagement rating on a scale of 1 to 5: mean =  
114 3.8, s.d. = 0.96, median = 4, median absolute deviation [m.a.d.] = 0.72; attention rating: mean =  
115 4.1, s.d. = 0.87, median = 4, m.a.d. = 0.66).

116 During a separate behavioral visit one week prior to the scan, participants completed  
117 several self-report questionnaires and behavioral tasks to assess personality traits and cognitive  
118 abilities (see Fig. 1a for a schematic of the experimental protocol). Our primary measure of interest  
119 was subscale A from the Green et al. Paranoid Thoughts Scale<sup>21</sup> (GPTS-A), henceforth referred to



120 as trait paranoia score. We administered this scale on a different day, and placed it amongst other  
121 tasks unrelated to paranoia, to minimize any priming effects or demand characteristics that might  
122 influence participants' eventual reactions to the narrative. Possible scores on the GPTS-A range  
123 from 16 to 80; higher scores are generally observed only in clinical populations<sup>21</sup>. In our healthy  
124 sample, we observed a right-skewed distribution that nonetheless had some variance (range = 16-  
125 40, mean = 20.6, s.d. = 6.3; median = 18.5, m.a.d. = 4.0; see Fig. 1b for a histogram of the  
126 distribution). This is consistent with observations from much larger sample sizes that trait paranoia  
127 follows an exponential, rather than normal, distribution in the healthy population<sup>5,6,21</sup>.

128

### 129 **Story listening evokes widespread neural synchrony**

130 Our primary approach for analyzing the fMRI data was inter-subject correlation (ISC),  
131 which is a model-free way to identify brain regions responding reliably to a naturalistic stimulus  
132 across subjects<sup>16,17</sup>. In this approach, the timecourse from each voxel in one subject's brain across  
133 the duration of the stimulus is correlated with the timecourse of the same voxel in a second  
134 subject's brain. Voxels that show high correlations in their timecourses across subjects are  
135 considered to have a stereotyped functional role in processing the stimulus. The advantage of this  
136 approach is that it does not require the investigator to have an *a priori* model of the task, nor to  
137 assume any fixed hemodynamic response function.

138 In a first-pass analysis, we calculated ISC at each voxel across the whole sample of  $n = 22$   
139 participants, using a recently developed statistical approach that relies on a linear mixed-effects  
140 model with crossed random effects to appropriately account for the correlation structure of the  
141 data<sup>22</sup>. Results are shown in Fig. 2. As expected given the audio-linguistic nature of the stimulus,  
142 ISC was highest in primary auditory cortex and language regions along the superior temporal lobe,  
143 but we also observed widespread ISC in other parts of association cortex, including frontal,  
144 parietal, midline and temporal areas, as well as the posterior cerebellum. These results replicate  
145 previous reports that complex naturalistic stimuli induce stereotyped responses across participants  
146 in not only the relevant primary cortex, but also higher-order brain regions<sup>15,16,23</sup>.

147 Also as expected, ISC was generally lower or absent in primary motor and somatosensory  
148 cortex, although we did observe significant ISC in parts of primary visual cortex, despite the fact  
149 that there was no timecourse of visual input during the story. (To encourage engagement, we had  
150 participants fixate on a static photograph that was thematically relevant to the story during

151 listening, so the observed ISC in visual cortex may reflect similarities in the timecourse of  
152 internally generated imagery across participants.)

153

### 154 **Paranoia modulates neural response to the narrative**

155 Having established that story listening evokes widespread neural synchrony across all  
156 participants, we next sought to determine if there were brain regions whose degree of ISC was  
157 modulated by trait paranoia. Using a median split of GPTS-A scores, we stratified our sample into  
158 a low-paranoia (GPTS-A  $\leq$  18,  $n = 11$ ) and high-paranoia (GPTS-A  $\geq$  19,  $n = 11$ ) group (Fig. 1b).  
159 We then used the same linear mixed-effects model described above formulated as a two-group  
160 contrast to reveal areas that are differentially synchronized across paranoia levels.

161 We opted for a median split rather than using raw paranoia score as a continuous covariate  
162 because of the unique challenge of an ISC-based analysis, which, to take advantage of all the  
163 information contained in the cross-subject correlation matrix (Fig. 1c), requires any covariates to  
164 be at the subject *pair* level, rather than the level of individual subjects. Because trait paranoia is a  
165 single scalar value per participant, it is difficult to calculate a meaningful pairwise metric. (Median  
166 splits can also mitigate the influence of extreme values, such as the two participants with GPTS-  
167 A  $\geq$  38 [cf. Fig. 1b], ensuring these do not have an outsize effect on the results.) Still, we conducted  
168 post-hoc tests to investigate continuous relationships with raw GPTS-A score whenever possible  
169 to respect the inherently continuous nature of this trait, and to facilitate interpretation.

170 We were primarily interested in three contrasts. First, which voxels show greater ISC  
171 among pairs of high-paranoia participants versus low-paranoia participants, or vice versa? Second  
172 and third, which voxels show greater ISC among pairs of low- or high-paranoia participants,  
173 respectively (i.e., low-low or high-high), than pairs of participants mismatched for group (i.e.,  
174 high-low)? All three contrasts reveals regions whose response timecourses are modulated by trait  
175 paranoia in some way. These contrasts are schematized in Fig. 1c.

176 Results are shown in Fig. 3. In the first contrast, several regions emerged as being more  
177 synchronized in the high-paranoia group relative to the low-paranoia group. Significant clusters  
178 were found in the left temporal pole (Talairach coordinates for center of mass: [+46.7, -10.0, -  
179 26.2]), left precuneus ([+10.8, +71.0, +35.9]), and two regions of the right medial prefrontal cortex  
180 (mPFC; one anterior [-8.1, -46.9, +16.3] and one dorsal [+2.9, -14.8, +45.1]; Fig. 3a). Searches for  
181 these coordinates on Neurosynth, an automated fMRI results synthesizer for mapping between

182 neural and cognitive states<sup>24</sup>, indicated that for the left temporal pole and right anterior mPFC  
183 clusters, top meta-analysis terms included “mentalizing”, “mental states”, “intentions”, and  
184 “theory mind”. There were no regions showing a statistically significant difference in the reverse  
185 direction (low-paranoia > high-paranoia).

186 In the second contrast (Fig. 3b, cool colors), pairs of low-paranoia participants were more  
187 synchronized than pairs of inter-group participants in the left lateral occipital gyrus (center of mass:  
188 [+31.3, +86.1, +14.0], Neurosynth: “objects”, “scene”, “encoding”), and in the third contrast (Fig.  
189 3b, warm colors), pairs of high-paranoia participants were more synchronized than pairs of inter-  
190 group participants in the right angular gyrus ([-44.8, +57.9, +37.9], Neurosynth: “beliefs”).  
191 Interestingly, there were no voxels of statistically significant overlap between the second and third  
192 contrasts, indicating that no single region had a timecourse that was equally synchronized within  
193 groups but qualitatively different between groups. Instead, for most of the regions that emerged  
194 from the three contrasts, the relationship between trait paranoia and timecourse synchrony is best  
195 expressed by the Anna Karenina principle: all paranoid participants are alike; all not-paranoid  
196 participants are not-paranoid in their own way (except in the lateral occipital gyrus, where it is the  
197 opposite).

198 As these regions were obtained via dichotomization into groups, we also conducted post-  
199 hoc tests to determine if ISC remained sensitive to finer-grained differences in trait paranoia. We  
200 were primarily interested in two regions that emerged from the first contrast, the left temporal pole  
201 and right medial PFC, since these are known from prior literature to be involved in theory of mind  
202 and mentalizing. To determine whether ISC in these regions scales monotonically with trait  
203 paranoia, we visualized the participant-by-participant ISC matrices with participants ordered by  
204 trait paranoia score (Fig. 4a. 4c). Visual inspection suggests a relatively continuous increase in ISC  
205 values as one moves down and to the right along the diagonal, which represents pairs of  
206 increasingly high-paranoia participants. To quantify this, we plotted each participant’s median ISC  
207 with all other participants (i.e., the median of each row of the ISC matrix) against their paranoia  
208 rank within the sample (i.e., 1–22; Fig. 4b and d). For both ROIs, participants with higher paranoia  
209 rank tended to have higher median ISC ( $r_s = 0.71$  and  $r_s = 0.63$  for the left temporal pole and right  
210 medial PFC, respectively; both  $p < 0.002$ ). We used paranoia rank rather than raw score to mitigate  
211 the influence of the two participants with extreme paranoia scores ( $\geq 38$ ; cf. Fig. 1b).

212

## 213 **Effects are specific to paranoia**

214 We conducted several control analyses to rule out the possibility that the observed group  
215 differences were driven by a factor other than trait paranoia. (For all analyses in this section, we  
216 checked for both categorical and continuous relationships with paranoia; full results are reported  
217 in Table 1.)

218 For example, if the high-paranoia participants have better overall attentional and cognitive  
219 abilities, they might simply be paying closer attention to the story, inflating ISC values but not  
220 necessarily because of selective attention to ambiguous or suspicious details. However, there were  
221 no differences between high- and low-paranoia participants on any of the cognitive tasks we  
222 administered (verbal IQ, vocabulary, fluid intelligence or working memory), making it unlikely  
223 that observed differences are due to trait-level differences in attention or cognition. As for state-  
224 level attention during the story, there was no relationship between paranoia and number of  
225 comprehension questions answered correctly, total word count during the recall task, or self-report  
226 measures of engagement and attention. We also explored potential imaging-based confounds, and  
227 found that paranoia was not related to amount of head motion during the scan (as measured by  
228 mean framewise displacement), number of censored frames, or temporal signal-to-noise ratio  
229 (tSNR). Paranoia groups did not differ in age or sex breakdown. Thus we are reasonably confident  
230 that the observed effects are driven by true trait-level differences in paranoia between individuals.

231

## 232 **Activity to mentalizing events scales with paranoia**

233 Results of the first contrast from the two-group ISC analysis indicated that certain brain  
234 regions showed a more stereotyped response in high-paranoia versus low-paranoia individuals.  
235 What features of the narrative were driving activity in these regions? In theory, ISC allows for  
236 reverse correlation, in which peaks of activation in a given region's timecourse are used to recover  
237 the stimulus events that evoked them<sup>16</sup>. In practice, this is often difficult. Especially with narrative  
238 stimuli, in which structure is built up over relatively long timescales<sup>15</sup>, it is challenging to pinpoint  
239 exactly which event—word, phrase, sentence—triggered an increase in BOLD activity.

240 Rather than rely on reverse correlation, a data-driven *decoding* approach, we took an  
241 *encoding* approach: we modeled events in the task that we hypothesized would stimulate differing  
242 interpretations across individuals, and evaluated the degree to which certain regions of interest  
243 (ROIs) responded to such events, using a general linear model (GLM) analysis. Specifically, we

244 labeled sentences in the story when the main character was experiencing an ambiguous (i.e.,  
245 possibly suspicious) social interaction, and/or sentences when she was explicitly reasoning about  
246 the intentions of other characters. For brevity, we refer to these timepoints as “mentalizing events.”  
247 In creating the regressor, all events were time-locked to the end of the last word of the labeled  
248 sentences, when participants are presumably evaluating information they just heard and integrating  
249 it into their situation model of the story.

250 We hypothesized that the two ROIs from the previous analysis known to be involved in  
251 theory-of-mind and mentalizing, the left temporal pole and right medial PFC, would be more active  
252 to mentalizing events in individuals with higher trait paranoia. We included two additional ROIs,  
253 the left temporo-parietal junction (TPJ) and left Heschl’s gyrus, as a positive and negative control,  
254 respectively. We selected the left TPJ as a positive control because of its well-established role in  
255 theory-of-mind and mentalizing processes, and the fact that it emerged as highly synchronized  
256 across all participants (cf. Fig. 2) but did not show a group difference (cf. Fig. 3); thus we  
257 hypothesized that this region should respond to mentalizing events in all participants, regardless  
258 of trait paranoia. Conversely, left Heschl’s gyrus (primary auditory cortex) should only respond to  
259 low-level acoustic properties of the stimulus and not show preferential activation to mentalizing  
260 events in either group or the sample as a whole. See Fig. 5a for ROI locations.

261 For each participant, we regressed the timecourse of each of these four ROIs against the  
262 mentalizing-events regressor and compared the resulting regression coefficients between groups  
263 (Fig. 5b). Compared to low-paranoia individuals, high-paranoia individuals showed stronger  
264 responses in both the left temporal pole (two-sample  $t(20) = 2.71$ ,  $p_{\text{adj}} = 0.014$ ) and right medial  
265 PFC ( $t(20) = 3.36$ ,  $p_{\text{adj}} = 0.007$ ). As hypothesized, responses in the left TPJ were strong across the  
266 whole sample (one-sample  $t(21) = 8.73$ ,  $p < 0.0001$ ), but there was no significant difference  
267 between groups in this ROI ( $t(20) = 0.67$ ,  $p_{\text{adj}} = 0.34$ ). Also as hypothesized, the sample as a whole  
268 did not show a significant response to these events in primary auditory cortex (one-sample  $t(21) =$   
269  $0.44$ ,  $p = 0.66$ ), and there was no group difference ( $t(20) = 0.47$ ,  $p_{\text{adj}} = 0.34$ ).

270 To confirm that these results hold if paranoia is treated as a continuous variable, we  
271 conducted additional post-hoc tests in which we correlated participants’ paranoia ranks and  
272 regression coefficients for all four ROIs (Fig. 4c). As expected, response to suspicious events was  
273 significantly related to paranoia rank in the left temporal pole ( $r_s = 0.57$ ,  $p = 0.005$ ) and right medial

274 PFC ( $r_s = 0.64$ ,  $p = 0.001$ ), but not in the left TPJ ( $r_s = -0.04$ ,  $p = 0.86$ ) or left Heschl's gyrus ( $r_s =$   
275  $0.02$ ,  $p = 0.95$ ).

276 As an additional control, to check that this effect was specific to mentalizing events and  
277 not just any sentence offset, we crated an inverse regressor comprising all *non*-mentalizing events  
278 (i.e., by flipping the binary labels from the mentalizing-events regressor, such that all sentences  
279 were labeled *except* those containing an ambiguous social interaction or explicit mentalizing as  
280 described above). There were no differences between paranoia groups in any of the four ROIs in  
281 response to non-mentalizing sentences (Fig. 4d), and no continuous relationships between  
282 regression coefficient and paranoia rank (Fig. 4e). This indicates that trait paranoia is associated  
283 with differential sensitivity of the left temporal pole and right medial PFC to not just any  
284 information, but specifically to socially ambiguous information that presumably triggers theory-  
285 of-mind processes.

286

### 287 **Paranoia modulates behavioral response to the narrative**

288 Having established that trait paranoia modulates individuals' brain responses to an  
289 ambiguous narrative, we next sought to determine if this trait also modulates their behavioral  
290 responses to the narrative. In other words, does trait-related (intrinsic) paranoia bear upon state-  
291 related (stimulus-evoked) paranoia? If the observed differences in neural activity propagate up to  
292 conscious perception and interpretation of the stimulus, then participants' subjective experiences  
293 of the narrative should also bear a signature of trait paranoia.

294 Immediately following the scan, participants completed a post-narrative battery that  
295 consisted of free-speech prompts followed by multiple-choice items to characterize their beliefs  
296 and feelings about the story. For the first item, participants were asked to retell the story in as much  
297 detail as they could remember, and their speech was recorded. Participants were allowed to speak  
298 for as long as they wished on whatever aspects of the story they chose. Without guidance from the  
299 experimenter, participants recalled the story in rich detail, speaking an average of 1,081 words  
300 (range = 399-3,185, s.d. = 610).

301 Audio recordings of participants' speech were transcribed and submitted to the language  
302 analysis software Linguistic Inquiry and Word Count<sup>25</sup> (LIWC). The output of LIWC is one vector  
303 per participant describing the percentage of speech falling into various semantic and syntactic  
304 categories. Example semantic categories are positive emotion ('love', 'nice'), money ('cash',



305 ‘owe’), and body (‘hands’, ‘face’), while syntactic categories correspond to parts of speech such  
306 as pronouns, adjectives and prepositions; there are 67 categories in total.

307 Using partial least-squares regression, we searched for relationships between speech  
308 features and trait paranoia score. More than 72 percent of the variance in paranoia score could be  
309 accounted for by the first component of speech features; the loadings of semantic and syntactic  
310 categories for this component are visualized in Fig. 6a. The feature with the highest positive  
311 loading—indicating a positive relationship with paranoia—was affiliation, a category of words  
312 describing social and familial relationships (e.g., ‘ally’, ‘friend’, ‘social’). Also associated with  
313 high trait paranoia was frequent use of adjectives as well as anxiety- and risk-related words (e.g.,  
314 ‘bad’, ‘crisis’); drives, a meta-category that includes words concerning affiliation, achievement,  
315 power, reward and risk; and health-related words (e.g., ‘clinic’, ‘fever’, ‘infected’; recall that the  
316 story featured a doctor treating patients in a remote village; cf. Supplementary Note 1). Features  
317 with strongly negative loadings—indicating an inverse relationship with paranoia—included male  
318 references (e.g., ‘him’, ‘his’, ‘man’, ‘father’); anger-related words (‘yell’, ‘annoyed’); function  
319 words (‘it’, ‘from’, ‘so’, ‘with’); and conjunctions (‘and’, ‘but’, ‘until’). Fig. 6b contains specific  
320 examples for selected categories from participants’ speech transcripts.

321 After the free-speech prompts, participants answered a series of multiple-choice questions  
322 (see Supplementary Table 1 for the full questionnaire). First, they were asked to rate the degree to  
323 which they were experiencing various emotions (suspicion, paranoia, sadness, happiness,  
324 confusion, anxiety, etc; 16 in total) on a scale from 1 to 5. Most of ratings skewed low—for  
325 example, the highest paranoia rating was 3, and only six subjects rated their paranoia level higher  
326 than 1. Interestingly, there was no significant correlation between trait paranoia score and self-  
327 reported paranoia ( $r_s = -0.02$ ,  $p = 0.91$ ) or suspicion ( $r_s = 0.11$ ,  $p = 0.62$ ) following the story. Neither  
328 were any of the other emotion ratings significantly correlated with trait-level paranoia (all  
329 uncorrected  $p > 0.12$ ; see Fig. 6c).

330 Second, participants were asked to rate the three central characters on six personality  
331 dimensions (trustworthy, impulsive, considerate, intelligent, likeable, naïve; see Supplementary  
332 Fig. 1a). Third, they were asked to rate the likelihood of each of six scenarios (see Supplementary  
333 Fig. 1b), and finally, to indicate (via forced-choice options) what they believed the main character  
334 would do next, as well as what they themselves would do in her situation.



335           None of the individual questionnaire items significantly correlated with trait paranoia.  
336   However, to facilitate comparison with the speech data, we submitted the questionnaire data to a  
337   second partial least-squares regression to search for multidimensional relationships. This analysis  
338   revealed a first component of questionnaire responses that accounted for 62 percent of the variance  
339   in trait paranoia (Supplementary Fig. 1c). Features with the highest positive loadings, indicating a  
340   positive relationship with paranoia, included certain answers about what individuals thought the  
341   main character might do next as well as what they would do in her place (e.g., escape from the  
342   situation), as well as feeling more uncomfortable and suspicious following the story. Features with  
343   the highest negative loadings, indicating an inverse relationship with paranoia, included feeling  
344   more amused, inspired and hopeful following the story, as well a tendency to agree with one of  
345   the scenarios (“Juan and the other villagers had not known anything about the disease before  
346   Carmen arrived”).

347           Overall, then, we found signatures of paranoia in story-evoked behavior using both free  
348   speech and self-report measures. Participants’ free speech was slightly more sensitive than their  
349   answers on the multiple-choice questionnaire. Self-report is a coarse measure that may suffer from  
350   response bias; behavior provides a richer feature set that allows for the discovery of more subtle  
351   associations. In studying nuanced individual differences, then, these results highlight the  
352   desirability of capturing behavior in both traditional and naturalistic ways.

353

## 354   **DISCUSSION**

355

356           Here we have shown that a personality trait can act as a lens, or “implicit prime”, through  
357   which individuals perceive ambiguous events, shaping both their neural and behavioral responses  
358   to an identical stimulus. Previous work using naturalistic tasks has shown that brain activity and  
359   behavioral responses are sensitive to experimenter instructions, i.e., an explicit prime<sup>19,20</sup>, or to the  
360   nature of the stimulus itself, i.e., whether it is more or less compelling or entertaining<sup>26-28</sup>. The  
361   present study extends these results in an important new direction, suggesting that there is  
362   substantial implicit variation in the brain’s response to a naturalistic stimulus that stems from trait-  
363   level individual differences.

364           Our results have implications for the neural correlates of both trait- and state-related  
365   paranoia. Those with higher trait paranoia may have more stereotyped brain responses because

366 suspicious and/or paranoid schemas come to mind more readily for these individuals; the idea that  
367 certain individuals tend to engage certain constructs more frequently across time and situations  
368 has been termed “chronic accessibility”<sup>29</sup>. The relative hyperactivity of theory-of-mind regions to  
369 mentalizing events in high-paranoia individuals fits with the conception of paranoia as “over-  
370 mentalizing”, or the tendency to excessively attribute (malevolent) intentions to other people’s  
371 actions<sup>30</sup>. Both regions of differential response, the temporal pole and medial PFC, are sometimes,  
372 but not always, reported in theory-of-mind tasks broadly construed; individual differences may at  
373 least partially explain the inconsistencies in the literature<sup>31</sup>.

374 While the present study included only healthy controls with subclinical paranoia, it may  
375 provide a useful starting point for the study of paranoid or persecutory delusions in schizophrenia  
376 and related illnesses. Delusions with a persecutory theme account for roughly 70-80 percent of all  
377 delusions. This high prevalence is stable across time<sup>32</sup> and geo-cultural factors<sup>33-36</sup>, suggesting a  
378 strong biological component. Persecutory delusions are also the type most strongly associated with  
379 anger and most likely to be acted upon, especially in a violent manner<sup>37</sup>. Thus, understanding the  
380 neurobiological basis of paranoid delusions is a critical problem in psychiatry.

381 But because delusions typically have a slow, insidious onset, it is nearly impossible to  
382 retrospectively recover triggering events in individual patients. A related challenge is that while  
383 thematically similar, each patient’s delusion is unique in its details. Thus it is difficult to devise  
384 material that will evoke comparable responses across patients. One solution is to craft a model  
385 context using a stimulus that is ambiguous yet controlled—i.e., identical across participants,  
386 permitting meaningful comparisons of time-locked evoked activity— such as the one used in this  
387 work. Paradigms such as this one may shed light on mechanisms of delusion formation and/or  
388 provide eventual diagnostic or prognostic value.

389 While there is little work investigating brain activity during naturalistic stimuli in  
390 psychiatric populations, a handful of studies have used such paradigms in autism, finding that  
391 autistic individuals are less synchronized with one another and with typically developing controls  
392 while watching movies of social interactions<sup>38-40</sup>. Notably, the degree of asynchrony scales with  
393 autism-spectrum phenotype severity in both the patient and control groups<sup>39</sup>. It is interesting to  
394 juxtapose these reports with the present results, in which individuals with a stronger paranoia  
395 phenotype were *more* synchronized during exposure to socially relevant material; ultimately, this  
396 fits with the notion of autism and psychosis as opposite ends of the same spectrum, involving

397 hypo- and hyper-mentalization, respectively<sup>41,42</sup>. Future studies should combine naturalistic  
398 stimuli with ISC-based analyses that cut across diagnostic labels to examine how neural responses  
399 vary across the full range of human phenotypes.

400 From a methodological perspective, much of the fMRI research on individual differences  
401 has shifted in recent years from measuring activation in task-based conditions to measuring  
402 functional connectivity, predominantly at rest<sup>43-47</sup>. Both paradigms suffer from limitations:  
403 traditional tasks are so tightly controlled that they often lack ecological validity; resting-state  
404 scans, on the other hand, are entirely unconstrained, making it difficult to separate signal from  
405 noise. Naturalistic tasks may be a happy medium for studying both group-level functional brain  
406 organization as well as individual differences<sup>48,49</sup>. We and others argue that such tasks could serve  
407 as a “stress test” to draw out individual variation in brain and behaviors of interest<sup>50-54</sup>, enhancing  
408 signal in the search for neuroimaging-based biomarkers and permitting more precise inferences  
409 about the sources of individual differences in neural activity.

## 410 **METHODS**

411

### 412 **Participants**

413 A total of 23 healthy volunteers participated in this study. Data from one participant was excluded  
414 due to excessive head motion and self-reported falling asleep during the last third of the narrative.  
415 Thus, the final data set used for analysis contained 22 participants (11 females; age range = 19-35  
416 years, mean = 27, s.d. = 4.4). All participants were right-handed, native speakers of English, with  
417 no history of neurological disease or injury, and were not on psychoactive medication at the time  
418 of scanning. All participants provided written informed consent in accordance with the  
419 Institutional Review Board of Yale University. The experiment took place over two visits to the  
420 laboratory. Participants were paid \$25 upon completion of the first visit (behavioral assessments)  
421 and \$75 upon completion of the second visit (MRI scan); all participants completed both visits.

422

### 423 **Stimulus**

424 An original narrative was written by author E.S.F. to serve as the stimulus for this experiment. For  
425 a synopsis of the story, see Supplementary Note 1. The full audio recording, as well as a complete  
426 transcript, are available in the “stimuli” directory at the following URL:  
427 <https://openneuro.org/datasets/ds001338/>. To mitigate confounds associated with education level  
428 or verbal IQ, we wrote the narrative text to be easy to comprehend, with a readability level of  
429 78.1/100 and a grade 5.5 reading level as calculated by the Flesch-Kinkaid Formula.

430

431 *Audio recording.* A male native speaker of English read the story aloud and his speech was  
432 recorded using high-quality equipment at Haskins Laboratories (New Haven, Conn.). The speaker  
433 was instructed to read in a natural, conversational tone, but without excess emotion. The final  
434 length of the audio recording was 21:50.

435

### 436 **Experimental protocol**

437 *Session 1: Behavior.* Approximately one week prior to the scan visit, participants came to the  
438 laboratory to complete a battery of self-report and behavioral tasks. While our primary measure of  
439 interest was the Green et al. Paranoid Thoughts Scale (GPTS)<sup>21</sup>, we also administered several other  
440 psychological scales and cognitive assessments, in part to help reduce any demand characteristics

441 that would allow participants to intuit the purpose of the study. We chose the GPTS because it  
442 provides a meaningful assessment of trait-level paranoia in clinical, but crucially, also subclinical  
443 and healthy populations. In a previous study, score on this scale best predicted feelings of  
444 persecution following immersion in a virtual-reality environment<sup>55</sup>. The full GPTS contains two  
445 subscales, A and B, which pertain to ideas of social reference and ideas of persecution,  
446 respectively. We focused on subscale A, as it produces a wider range of scores in subclinical  
447 populations<sup>21</sup>.

448

449 The following cognitive tests were administered via the web interface of the University of  
450 Pennsylvania Computerized Neuropsychological Test Battery (PennCNP;  
451 [penncnp.med.upenn.edu](http://penncnp.med.upenn.edu))<sup>56</sup>: SRAVEN (short Raven's progressive matrices, a measure of  
452 abstraction and mental flexibility, or fluid intelligence); SPVRT (short Penn logical reasoning test,  
453 a measure of verbal intelligence); and LNB2 (letter n-back, a measure of working memory). We  
454 also administered the word reading test from the Wide Range Achievement Test 3 (WRAT)<sup>57</sup>, a  
455 measure of reading and vocabulary.

456

457 *Session 2: MRI scan.* The full audio recording was divided into three segments of length 8:46,  
458 7:32, and 5:32, respectively; each of these segments was delivered in a continuous functional run  
459 while participants were in the scanner. To ensure attention, after each run, subjects answered three  
460 challenging multiple-choice comprehension questions regarding the content of the part they had  
461 just heard, for a total of nine questions. Immediately upon exiting the scanner, participants  
462 completed a post-narrative questionnaire that consisted of open-ended prompts to elicit free  
463 speech, followed by multiple-choice items. These are described further below.

464

### 465 **MRI data acquisition and preprocessing**

466 Scans were performed on a 3T Siemens TimTrio system at the Yale Magnetic Resonance  
467 Research Center. After an initial localizing scan, a high-resolution 3D volume was collected using  
468 a magnetization prepared rapid gradient echo (MPRAGE) sequence (208 contiguous sagittal slices,  
469 slice thickness = 1 mm, matrix size 256 × 256, field of view = 256 mm, TR = 2400 ms, TE = 1.9  
470 ms, flip angle = 8°). Functional images were acquired using a multiband T2\*-sensitive gradient-  
471 recalled single shot echo-planar imaging pulse sequence (TR = 1000 ms, TE = 30 ms, voxel size

472 = 2.0mm<sup>3</sup>, flip angle = 60°, bandwidth = 1976 Hz/pixel, matrix size = 110 × 110, field of view =  
473 220 mm × 220 mm, multiband factor = 4).

474 We acquired the following functional scans: 1) an initial eyes-open resting-state run  
475 (6:00/360 TRs in duration) during which subjects were instructed to relax and think of nothing in  
476 particular; 2) a movie-watching run using Inscapes<sup>58</sup> (7:00/420 TRs); 3) three narrative-listening  
477 runs corresponding to parts 1, 2 and 3 of the story (21:50/1310 TRs in total); and 4) a post-  
478 narrative, eyes-open resting-state run (6:00/360 TRs) during which subjects were instructed to  
479 reflect on the story they had just heard. The present work focuses exclusively on data acquired  
480 during narrative listening. The narrative stimulus was delivered through MRI-compatible audio  
481 headphones and a short “volume check” scan was conducted just prior to the first narrative run to  
482 ensure that participants could adequately hear the stimulus above the scanner noise. To promote  
483 engagement, during the three narrative runs, participants were asked to fixate on a static image of  
484 a jungle settlement and to actively imagine the story events as they unfolded.

485 Following conversion of the original DICOM images to NIFTI format, AFNI (Cox 1996)  
486 was used to preprocess MRI data. The functional time series went through the following  
487 preprocessing steps: despiking, head motion correction, affine alignment with anatomy, nonlinear  
488 alignment to a Talairach template (TT\_N27), and smoothing with an isotropic FWHM of 5 mm.  
489 A ventricle mask was defined on the template and intersected with the subject’s cerebrospinal fluid  
490 (CSF) mask to make a subject-specific ventricle mask. Regressors were created from the first three  
491 principal components of the ventricles, and fast ANATICOR (Jo et al 2010) was implemented to  
492 provide local white matter regressors. Additionally, the subject’s 6 motion time series, their  
493 derivatives and linear polynomial baselines for each of the functional runs were included as  
494 regressors. Censoring of time points was performed whenever the per-time motion (Euclidean  
495 norm of the motion derivatives) was  $\geq 0.3$  or when  $\geq 10\%$  of the brain voxels were outliers.  
496 Censored time points were set to zero rather than removed altogether (this is the conventional way  
497 to do censoring, but especially important for inter-subject correlation analyses, to preserve the  
498 temporal structure across participants). The final output of this preprocessing pipeline was a single  
499 functional run concatenating data from the three story runs (total duration = 21:50, 1310 TRs). All  
500 analyses were conducted in volume space and projected to the surface for visualization purposes.

501 We used mean framewise displacement (MFD), a per-participant summary metric, to  
502 assess the amount of head motion in the sample. MFD was overall relatively low (after censoring:

503 mean = 0.075 mm, s.d. = 0.026, range = 0.035-0.14). Number of censored time points during the  
504 story was overall low but followed a right-skewed distribution (range = 0-135, median = 4, median  
505 absolute deviation = 25). All 22 participants in the final analysis retained at least 89 percent of the  
506 total time points in the story, so missing data was not a substantial concern. Still, we performed  
507 additional control analyses to ensure that number of censored timepoints and amount of head  
508 motion were not associated with paranoia score in any way that would confound interpretation of  
509 the results (see Table 1).

510

### 511 **Inter-subject correlation**

512 Following preprocessing, inter-subject correlation (ISC) during the story was computed  
513 across all possible pairs of subjects ( $i,j$ ) using AFNI's 3dTcorrelate function, resulting in 231  
514 ( $n*(n-1)/2$ , where  $n = 22$ ) unique ISC maps, where the value at each voxel represents the Pearson's  
515 correlation between that voxel's timecourse in subject  $i$  and its timecourse in subject  $j$ .

516 To identify voxels demonstrating statistically significant ISC across all 231 subject pairs,  
517 we performed inference at the single-group level using a recently developed linear mixed-effects  
518 (LME) model with a crossed random-effects formulation to accurately account for the correlation  
519 structure embedded in the ISC data<sup>22</sup>. This approach has been characterized extensively, including  
520 a comparison to non-parametric approaches, and found to demonstrate proper control for false  
521 positives and good power attainment<sup>22</sup>. The resulting map was corrected for multiple comparisons  
522 and thresholded for visualization using a voxelwise false discovery rate threshold of  $q < 0.001$   
523 (Fig. 2).

524 In a second analysis, we stratified participants according to a median split of scores on the  
525 GPTS-A subscale. We used these groups to identify voxels that had higher ISC values within one  
526 paranoia group or the other, or higher ISC values within rather than across paranoia groups. To  
527 this end, we used a two-group formulation of the LME model. This model gives the following  
528 outputs: voxelwise population ISC values within group 1 ( $G_{11}$ ); voxelwise population ISC values  
529 within group 2 ( $G_{22}$ ); voxelwise population ISC values between the two groups that reflect the ISC  
530 effect between any pair of subjects with each belonging to different groups ( $G_{12}$ ). These outputs  
531 can be compared to obtain several possible contrasts. Here, we were primarily interested in three  
532 of these contrasts: 1)  $G_{11}$  versus  $G_{22}$ , 2)  $G_{11}$  versus  $G_{12}$ , and 3)  $G_{22}$  versus  $G_{12}$ . The maps resulting  
533 from each of these contrasts were thresholded using an initial voxelwise threshold of  $p < 0.002$



534 and controlled for family-wise error (FWE) using a cluster size threshold of 50 voxels,  
535 corresponding to a corrected  $p$ -value of 0.05. We opted for a particularly stringent initial  $p$ -  
536 threshold in light of recent concerns about false positives arising from performing cluster  
537 correction on maps with more lenient initial thresholds<sup>59</sup>.

538

### 539 **Event-related analysis**

540 *Creating the regressor.* A forced-aligner (Gentle; <https://lowerquality.com/gentle/>) was  
541 used to obtain precise timing information for each word in the narrative, by aligning the audio file  
542 with its transcript. One of the authors (E.S.F.) manually labeled sentences containing either an  
543 ambiguous social interaction or an instance of the main character mentalizing about other  
544 characters' intentions using a binary scoring system (1 = ambiguous social interaction or  
545 mentalizing present in sentence, 0 = neither ambiguous social interaction nor mentalizing present).  
546 Four additional, independent raters previously naïve to the narrative listened to the same version  
547 that was played to participants in the scanner. They were then given a written version of the  
548 narrative broken down by sentence and asked to label each sentence as described above. Sentences  
549 that were labeled by at least three of the five raters were included in the final set of events. There  
550 were 48 sentences that met this criteria, with 17, 13 and 18 occurring in parts 1, 2 and 3 of the  
551 narrative, respectively.

552 Events were timestamped based on the TR corresponding to the offset of the last word of  
553 each labeled sentence. These timestamps were convolved with a canonical hemodynamic response  
554 function (HRF) to create the mentalizing-events regressor. Our assumption that evaluation and  
555 integration would happen primarily at the end of the sentence was based on theories of text  
556 comprehension, which hold that readers/listeners segment continuous linguistic information online  
557 into larger units of meaning, or “macropropositions”; the mental models that listeners use to  
558 represent narratives are thus updated primarily at event boundaries<sup>60-62</sup>. Empirical neurobiological  
559 support for this comes from Whitney et al.<sup>63</sup>, who showed, using a 23-minute continuous narrative  
560 stimulus, that sentence boundaries coinciding with narrative shifts—defined as shifts in character,  
561 time, location, or action— evoked more brain activity than sentence boundaries not coincident  
562 with such shifts. Additional neuroimaging evidence comes from Zacks et al.<sup>64</sup>, who demonstrated  
563 transient changes in brain activity that were time-locked to event boundaries during movie  
564 viewing.

565           However, some degree of evaluation and integration could also be happening online as  
566 participants listen to the event, and ideally the results from the regression would not depend on  
567 methodological choices about which parts of the sentence to model. To test this, we created a  
568 second version of the regressor, this time treating the entire sentence as a mini-block by modeling  
569 all TRs in each of the labeled sentences. Results were unchanged (see Supplementary Fig. 2). Thus  
570 we are confident that the results are robust to this methodological choice.

571           As a control analysis, we also created a regressor that was the inverse of the above  
572 regressor, by flipping the binary labels (0 or 1) for all sentences and convolving the corresponding  
573 sentences offset timestamps with the HRF; we refer to this as the non-mentalizing-events  
574 regressor.

575           *ROI definition and GLM.* For the left temporal pole and right medial PFC, ROIs were  
576 defined based on the cluster-corrected group-comparison map for the contrast  $ISC_{high} > ISC_{low}$  (cf.  
577 Fig. 3a). For the left temporo-parietal junction (TPJ) and left Heschl's gyrus, spherical ROIs were  
578 created by placing a sphere with radius 4 mm around a central coordinate. In the case of the TPJ  
579 this was the peak voxel in this region identified by the whole-sample ISC analysis (cf. Fig. 2;  
580 Talairach *xyz*, [+53, +55, +18]). In the case of Heschl's gyrus, this was selected anatomically  
581 (Talairach *xyz*, [-41, -24, +9]; as in Schönwiesner et al.<sup>65</sup>).

582           Timecourses for each ROI were extracted from each participant's preprocessed functional  
583 data using AFNI's 3dmaskave function and regressed against both the mentalizing- and non-  
584 mentalizing-events regressors to obtain a regression coefficient for each participant for each ROI.  
585 These regression coefficients were then compared across groups using two-sample t-tests corrected  
586 for four multiple comparisons. In the case of the two control ROIs (TPJ and Heschl's gyrus) for  
587 the mentalizing-events regressor, these coefficients were also pooled across both groups and  
588 submitted to a one-sample t-test to test for a significant deviation from zero.

589

## 590 **Free speech capture**

591           Immediately following their exit from the scanner, we gave participants the following  
592 prompts and recorded their speech: (1) "Please retell the story in as much detail as you can  
593 remember"; and (2) "What did you think of the story as a whole? In particular, did anything strike  
594 you as strange or confusing? How do you feel after listening to the story?" Here we focus on data  
595 acquired from the first prompt, as participants consistently talked for much longer to this one than

596 to the second one (since they tended to preempt answers to second prompt in their answer to the  
597 first).

598

### 599 **Multiple-choice questionnaire**

600 Following the free-speech prompts, we had participants complete a computerized multiple-  
601 choice questionnaire to assess their feelings toward and beliefs about the story. A full list of items  
602 is provided in Supplementary Table 1; there were 47 in total.

603

### 604 **Analysis of speech features**

605 Audio recordings of participants' retelling of the story were professionally transcribed by  
606 a third-party company. We submitted the resulting transcripts to Linguistic Inquiry and Word  
607 Count (LIWC; [www.liwc.net](http://www.liwc.net))<sup>25</sup>, a software program that takes as input a given text and counts the  
608 percentage of words falling into different syntactic and semantic categories. Because LIWC was  
609 developed by researchers with interests in social, clinical, health, and cognitive psychology, the  
610 language categories were created to capture people's social and psychological states.

611 We restricted LIWC output to the 67 linguistic (syntactic and semantic) categories,  
612 excluding categories relating to metadata (e.g., percentage of words found in the LIWC  
613 dictionary), as well as categories irrelevant to spoken language (e.g., punctuation). Thus, our final  
614 LIWC output was a 22x67 matrix where each row corresponds to a participant and each column  
615 to a category.

616 These categories can be scaled very differently from one another. For example, words in  
617 the syntactic category "pronoun" accounted for between 10.3-20.5 percent of speech transcripts,  
618 while words in the semantic category "leisure" accounted for only 0-1.09 percent. To give  
619 approximately equal weight to all categories, we standardized each category (to have zero mean  
620 unit variance) across participants before performing partial least squares regression (PLSR) as  
621 described in the next section. This ensures that the resulting PLS components are not simply  
622 dominated by variance in categories that are represented heavily in all human speech.

623

### 624 **Relating story-evoked behavior to paranoia**

625 To determine which speech features were most related to trait paranoia, we submitted the  
626 data to a partial least squares regression (PLSR) with the z-scored speech features as X (predictors)

627 and trait paranoia score as Y (response), implemented in Matlab as *plsregress*. PLSR is a latent  
628 variable approach to modeling the covariance structure between two matrices, which seeks to find  
629 the direction in X space that explains the maximum variance in Y space. It is well suited to the  
630 current problem, because it can handle a predictor matrix with more variables than observations,  
631 as well as multi-collinearity among the predictors.

632 In a first-pass analysis, we ran a model with 10 components to determine the number of  
633 components needed to explain most of the variance in trait paranoia. Results of this analysis  
634 indicated that the first component was sufficient to explain 72.3 percent of the total variance in  
635 paranoia score, so we selected just this component for visualization and interpretation. Feature  
636 loadings for this component are visualized in Fig. 6a.

637 In a parallel analysis, we submitted participants' answers to the multiple-choice  
638 questionnaire to a PLSR as the X (predictor) matrix, again with paranoia score as the Y (response)  
639 variable. Results of this analysis indicated that the first component was sufficient to explain 61.5  
640 percent of the variance in paranoia score. Feature loadings for this component are visualized in  
641 Supplementary Fig. 1c.

642

#### 643 **Data availability**

644 Source data generated during this study, including raw MRI data and the full narrative  
645 stimulus (audio and text), are available at: [<https://openneuro.org/datasets/ds001338/>].

646

#### 647 **Code availability**

648 More information about this project, including links to code and other supporting material,  
649 can be found at: [<https://esfinn.github.io/projects/ParanoiaStory.html>].

650

- 651  
652  
653 1 Davis, B., Anderson, R. & Walls, J. *Rashomon Effects: Kurosawa, Rashomon and Their*  
654 *Legacies*. (Taylor & Francis, 2015).  
655 2 Savulich, G., Freeman, D., Shergill, S. & Yiend, J. Interpretation Biases in Paranoia.  
656 *Behav. Ther.* **46**, 110-124, (2015).  
657 3 Johns, L. C. & Van Os, J. The Continuity of Psychotic Experiences in the General  
658 Population. *Clin. Psychol. Rev.* **21**, 1125-1141, (2001).  
659 4 Insel, T. *et al.* Research Domain Criteria (Rdoc): Toward a New Classification Framework  
660 for Research on Mental Disorders. *Am. J. Psychiatry.* **167**, 748-751, (2010).  
661 5 Freeman, D. *et al.* Psychological Investigation of the Structure of Paranoia in a Non-  
662 Clinical Population. *The British Journal of Psychiatry* **186**, 427-435, (2005).  
663 6 Bebbington, P. E. *et al.* *The Structure of Paranoia in the General Population*. Vol. 202  
664 (2013).  
665 7 Whalley, H. C. *et al.* Correlations between Fmri Activation and Individual Psychotic  
666 Symptoms in Un-Medicated Subjects at High Genetic Risk of Schizophrenia. *BMC*  
667 *Psychiatry* **7**, 61, (2007).  
668 8 Brent, B. K. *et al.* Subclinical Delusional Thinking Predicts Lateral Temporal Cortex  
669 Responses During Social Reflection. *Soc. Cogn. Affect. Neurosci.*, nss129, (2012).  
670 9 Sumich, A., Castro, A. & Kumari, V. N100 and N200, but Not P300, Amplitudes Predict  
671 Paranoia/Suspiciousness in the General Population. *Pers. Individ. Dif.* **61**, 74-79, (2014).  
672 10 Modinos, G., Renken, R., Ormel, J. & Aleman, A. Self-Reflection and the Psychosis-Prone  
673 Brain: An Fmri Study. *Neuropsychology* **25**, 295-305, (2011).  
674 11 Modinos, G. *et al.* Multivariate Pattern Classification Reveals Differential Brain Activation  
675 During Emotional Processing in Individuals with Psychosis Proneness. *Neuroimage* **59**,  
676 3033-3041, (2012).  
677 12 Bishop, S. J. Neural Mechanisms Underlying Selective Attention to Threat. *Ann. N. Y.*  
678 *Acad. Sci.* **1129**, 141-152, (2008).  
679 13 Kukkonen, K. Bayesian Narrative: Probability, Plot and the Shape of the Fictional World.  
680 *Anglia* **132**, 720-739, (2014).  
681 14 Mar, R. A. The Neural Bases of Social Cognition and Story Comprehension. *Annu. Rev.*  
682 *Psychol.* **62**, 103-134, (2011).  
683 15 Lerner, Y., Honey, C. J., Silbert, L. J. & Hasson, U. Topographic Mapping of a Hierarchy  
684 of Temporal Receptive Windows Using a Narrated Story. *J. Neurosci.* **31**, 2906-2915,  
685 (2011).  
686 16 Hasson, U., Nir, Y., Levy, I., Fuhrmann, G. & Malach, R. Intersubject Synchronization of  
687 Cortical Activity During Natural Vision. *Science* **303**, 1634-1640, (2004).  
688 17 Hasson, U., Malach, R. & Heeger, D. J. Reliability of Cortical Activity During Natural  
689 Stimulation. *Trends in Cognitive Sciences* **14**, 40-48, (2010).  
690 18 Cooper, E. A., Hasson, U. & Small, S. L. Interpretation-Mediated Changes in Neural  
691 Activity During Language Comprehension. *Neuroimage* **55**, 1314-1323, (2011).  
692 19 Lahnakoski, J. M. *et al.* Synchronous Brain Activity across Individuals Underlies Shared  
693 Psychological Perspectives. *Neuroimage* **100**, 316-324, (2014).  
694 20 Yeshurun, Y. *et al.* Same Story, Different Story: The Neural Representation of Interpretive  
695 Frameworks. *Psychol. Sci.* **28**, 307-319, (2017).

- 696 21 Green, C. *et al.* Measuring Ideas of Persecution and Social Reference: The Green Et Al.  
697 Paranoid Thought Scales (Gpts). *Psychol. Med.* **38**, 101-111, (2008).
- 698 22 Chen, G., Taylor, P. A., Shin, Y.-W., Reynolds, R. C. & Cox, R. W. Untangling the  
699 Relatedness among Correlations, Part II: Inter-Subject Correlation Group Analysis through  
700 Linear Mixed-Effects Modeling. *NeuroImage* **147**, 825-840, (2017).
- 701 23 Yarkoni, T., Speer, N. K. & Zacks, J. M. Neural Substrates of Narrative Comprehension  
702 and Memory. *Neuroimage* **41**, 1408-1425, (2008).
- 703 24 Yarkoni, T., Poldrack, R. A., Nichols, T. E., Van Essen, D. C. & Wager, T. D. Large-Scale  
704 Automated Synthesis of Human Functional Neuroimaging Data. *Nature Methods* **8**, 665,  
705 (2011).
- 706 25 Linguistic Inquiry and Word Count: Liwc 2015 (Pennebaker Conglomerates, Austin, TX,  
707 2015).
- 708 26 Schmäzle, R., Häcker, F. E. K., Honey, C. J. & Hasson, U. Engaged Listeners: Shared  
709 Neural Processing of Powerful Political Speeches. *Soc. Cogn. Affect. Neurosci.* **10**, 1137-  
710 1143, (2015).
- 711 27 Dmochowski, J. P. *et al.* Audience Preferences Are Predicted by Temporal Reliability of  
712 Neural Processing. *Nature communications* **5**, 4567, (2014).
- 713 28 Ki, J. J., Kelly, S. P. & Parra, L. C. Attention Strongly Modulates Reliability of Neural  
714 Responses to Naturalistic Narrative Stimuli. *J. Neurosci.* **36**, 3092-3101, (2016).
- 715 29 Higgins, E. T., King, G. A. & Mavin, G. H. Individual Construct Accessibility and  
716 Subjective Impressions and Recall. *J. Pers. Soc. Psychol.* **43**, 35, (1982).
- 717 30 Brüne, M. "Theory of Mind" in Schizophrenia: A Review of the Literature. *Schizophr.*  
718 *Bull.* **31**, 21-42, (2005).
- 719 31 Carrington, S. J. & Bailey, A. J. Are There Theory of Mind Regions in the Brain? A Review  
720 of the Neuroimaging Literature. *Hum. Brain Mapp.* **30**, 2313-2335, (2009).
- 721 32 Cannon, B. J. & Kramer, L. M. Delusion Content across the 20th Century in an American  
722 Psychiatric Hospital. *Int. J. Soc. Psychiatry* **58**, 323-327, (2012).
- 723 33 Tateyama, M., Asai, M., Hashimoto, M., Bartels, M. & Kasper, S. Transcultural Study of  
724 Schizophrenic Delusions. Tokyo Versus Vienna and Tübingen (Germany).  
725 *Psychopathology* **31**, 59-68, (1997).
- 726 34 Stompe, T. *et al.* Comparison of Delusions among Schizophrenics in Austria and in  
727 Pakistan. *Psychopathology* **32**, 225-234, (1998).
- 728 35 Gutiérrez-Lobos, K., Schmid-Siegel, B., Bankier, B. & Walter, H. Delusions in First-  
729 Admitted Patients: Gender, Themes and Diagnoses. *Psychopathology*, (2001).
- 730 36 Brakoulias, V. & Starcevic, V. A Cross-Sectional Survey of the Frequency and  
731 Characteristics of Delusions in Acute Psychiatric Wards. *Australasian Psychiatry* **16**, 87-  
732 91, (2008).
- 733 37 Coid, J. W., Ullrich, S., Kallis, C. & *et al.* The Relationship between Delusions and  
734 Violence: Findings from the East London First Episode Psychosis Study. *JAMA Psychiatry*  
735 **70**, 465-471, (2013).
- 736 38 Hasson, U. *et al.* Shared and Idiosyncratic Cortical Activation Patterns in Autism Revealed  
737 under Continuous Real-Life Viewing Conditions. *Autism Research* **2**, 220-231, (2009).
- 738 39 Salmi, J. *et al.* The Brains of High Functioning Autistic Individuals Do Not Synchronize  
739 with Those of Others. *NeuroImage: Clinical* **3**, 489-497, (2013).



- 740 40 Byrge, L., Dubois, J., Tyszka, J. M., Adolphs, R. & Kennedy, D. P. Idiosyncratic Brain  
741 Activation Patterns Are Associated with Poor Social Comprehension in Autism. *J.*  
742 *Neurosci.* **35**, 5837-5850, (2015).
- 743 41 Crespi, B. & Badcock, C. Psychosis and Autism as Diametrical Disorders of the Social  
744 Brain. *Behav. Brain Sci.* **31**, 241-261, (2008).
- 745 42 Ciaramidaro, A. *et al.* Schizophrenia and Autism as Contrasting Minds: Neural Evidence  
746 for the Hypo-Hyper-Intentionality Hypothesis. *Schizophr. Bull.* **41**, 171-179, (2015).
- 747 43 Kelly, C., Biswal, B. B., Craddock, R. C., Castellanos, F. X. & Milham, M. P.  
748 Characterizing Variation in the Functional Connectome: Promise and Pitfalls. *Trends in*  
749 *Cognitive Sciences* **16**, 181-188, (2012).
- 750 44 Castellanos, F. X., Di Martino, A., Craddock, R. C., Mehta, A. D. & Milham, M. P. Clinical  
751 Applications of the Functional Connectome. *Neuroimage* **80**, 527-540, (2013).
- 752 45 Finn, E. S. *et al.* Functional Connectome Fingerprinting: Identifying Individuals Using  
753 Patterns of Brain Connectivity. *Nat. Neurosci.* **18**, 1664-1671, (2015).
- 754 46 Smith, S. M. *et al.* A Positive-Negative Mode of Population Covariation Links Brain  
755 Connectivity, Demographics and Behavior. *Nat. Neurosci.* **18**, 1565-1567, (2015).
- 756 47 Rosenberg, M. D. *et al.* A Neuromarker of Sustained Attention from Whole-Brain  
757 Functional Connectivity. *Nat. Neurosci.* **advance online publication**, (2015).
- 758 48 Ren, Y., Nguyen, V. T., Guo, L. & Guo, C. C. Inter-Subject Functional Correlation Reveal  
759 a Hierarchical Organization of Extrinsic and Intrinsic Systems in the Brain. *Sci. Rep.* **7**,  
760 10876, (2017).
- 761 49 Vanderwal, T. *et al.* Individual Differences in Functional Connectivity During Naturalistic  
762 Viewing Conditions. *bioRxiv*, (2016).
- 763 50 Finn, E. S. & Constable, R. T. Individual Variation in Functional Brain Connectivity:  
764 Implications for Personalized Approaches to Psychiatric Disease. *Dialogues Clin.*  
765 *Neurosci.* **18**, 277-287, (2016).
- 766 51 Dubois, J. & Adolphs, R. Building a Science of Individual Differences from Fmri. *Trends*  
767 *in Cognitive Sciences* **20**, 425-443, (2016).
- 768 52 Koyama, M. S. *et al.* Imaging the at-Risk Brain: Future Directions. *J. Int. Neuropsychol.*  
769 *Soc.* **22**, 164-179, (2016).
- 770 53 Finn, E. S. *et al.* Can Brain State Be Manipulated to Emphasize Individual Differences in  
771 Functional Connectivity? *Neuroimage*, (2017).
- 772 54 Guo, C. C., Hyett, M. P., Nguyen, V. T., Parker, G. B. & Breakspear, M. J. Distinct  
773 Neurobiological Signatures of Brain Connectivity in Depression Subtypes During Natural  
774 Viewing of Emotionally Salient Films. *Psychol. Med.* **46**, 1535-1545, (2016).
- 775 55 VALMAGGIA, L. R. *et al.* Virtual Reality and Paranoid Ideations in People with an 'at-  
776 Risk Mental State' for Psychosis. *The British Journal of Psychiatry* **191**, s63-s68, (2007).
- 777 56 Gur, R. C. *et al.* Computerized Neurocognitive Scanning:: I. Methodology and Validation  
778 in Healthy People. *Neuropsychopharmacology* **25**, 766-776, (2001).
- 779 57 Wilkinson, G. S. *Wrat-3: Wide Range Achievement Test Administration Manual.* (Wide  
780 Range, Incorporated, 1993).
- 781 58 Vanderwal, T., Kelly, C., Eilbott, J., Mayes, L. C. & Castellanos, F. X. Inscapes: A Movie  
782 Paradigm to Improve Compliance in Functional Magnetic Resonance Imaging.  
783 *Neuroimage* **122**, 222-232, (2015).
- 784 59 Eklund, A., Nichols, T. E. & Knutsson, H. Cluster Failure: Why Fmri Inferences for Spatial  
785 Extent Have Inflated False-Positive Rates. *Proc. Natl. Acad. Sci. USA*, 201602413, (2016).



786 60 Zwaan, R. A. & Radvansky, G. A. Situation Models in Language Comprehension and  
787 Memory. *Psychol. Bull.* **123**, 162-185, (1998).  
788 61 Johnson-Laird, P. (Cambridge, MA: Harvard University Press, 1983).  
789 62 Van Dijk, T. A., Kintsch, W. & Van Dijk, T. A. *Strategies of Discourse Comprehension*.  
790 (Academic Press New York, 1983).  
791 63 Whitney, C. *et al.* Neural Correlates of Narrative Shifts During Auditory Story  
792 Comprehension. *Neuroimage* **47**, 360-366, (2009).  
793 64 Zacks, J. M. *et al.* Human Brain Activity Time-Locked to Perceptual Event Boundaries.  
794 *Nat. Neurosci.* **4**, 651, (2001).  
795 65 Schönwiesner, M. *et al.* Heschl's Gyrus, Posterior Superior Temporal Gyrus, and Mid-  
796 Ventrolateral Prefrontal Cortex Have Different Roles in the Detection of Acoustic  
797 Changes. *J. Neurophysiol.* **97**, 2075-2082, (2007).  
798  
799

800 **Acknowledgements**

801 This research was supported by a National Science Foundation Graduate Research Fellowship to  
802 E.S.F., and by the Intramural Research Program of the NIMH (annual report ZIAMH002783).  
803 Portions of this study used the computational capabilities of the NIH HPC Biowulf cluster  
804 (*biowulf.nih.gov*). The authors thank Paul Taylor for advice on preprocessing pipelines for  
805 naturalistic task data, Richard Betzel for sharing code to visualize component feature loadings  
806 (Fig. 6a and Supplementary Fig. 2), and Javier Gonzalez-Castillo, Daniel Handwerker, David  
807 Jangraw, Peter Molfese, Monica Rosenberg, and Tamara Vanderwal for helpful discussion.

808

809 **Author contributions**

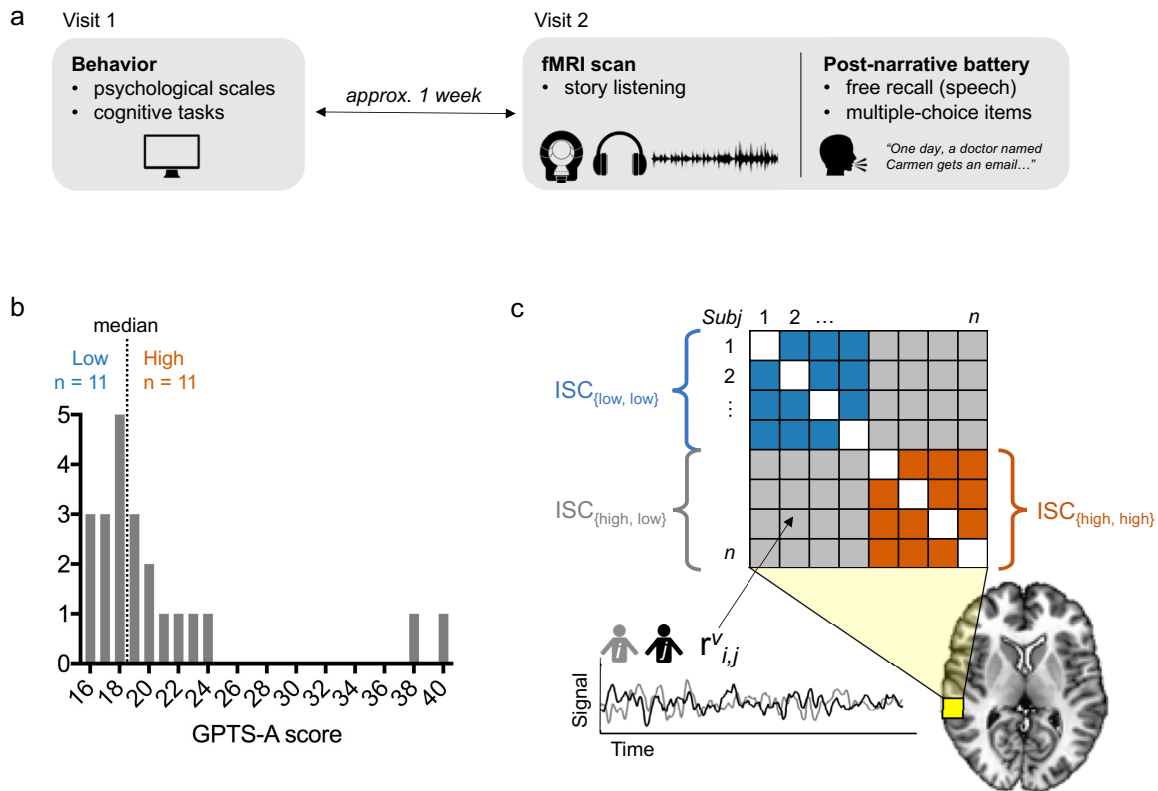
810 E.S.F, P.R.C and R.T.C conceived the study. E.S.F. developed experimental materials and  
811 performed data collection. E.S.F. and G.C. analyzed the data. E.S.F., P.R.C., P.A.B. and R.T.C  
812 interpreted results. E.S.F. wrote the manuscript with comments from all other authors.

813

814 **Competing financial interests**

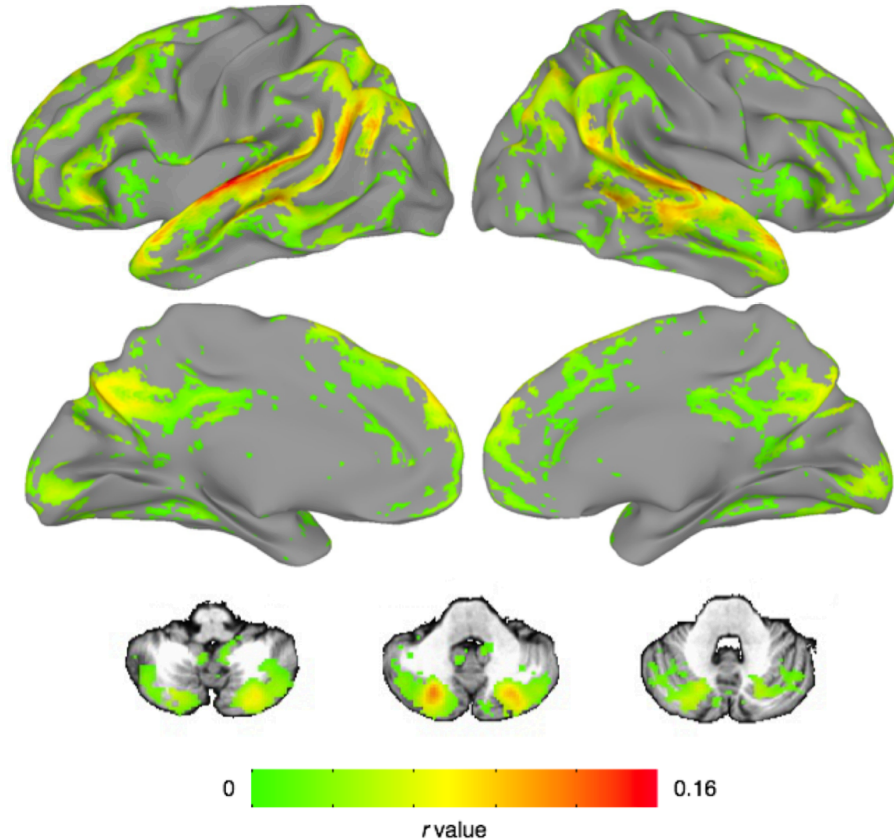
815 The authors have no competing financial interests to declare.

816



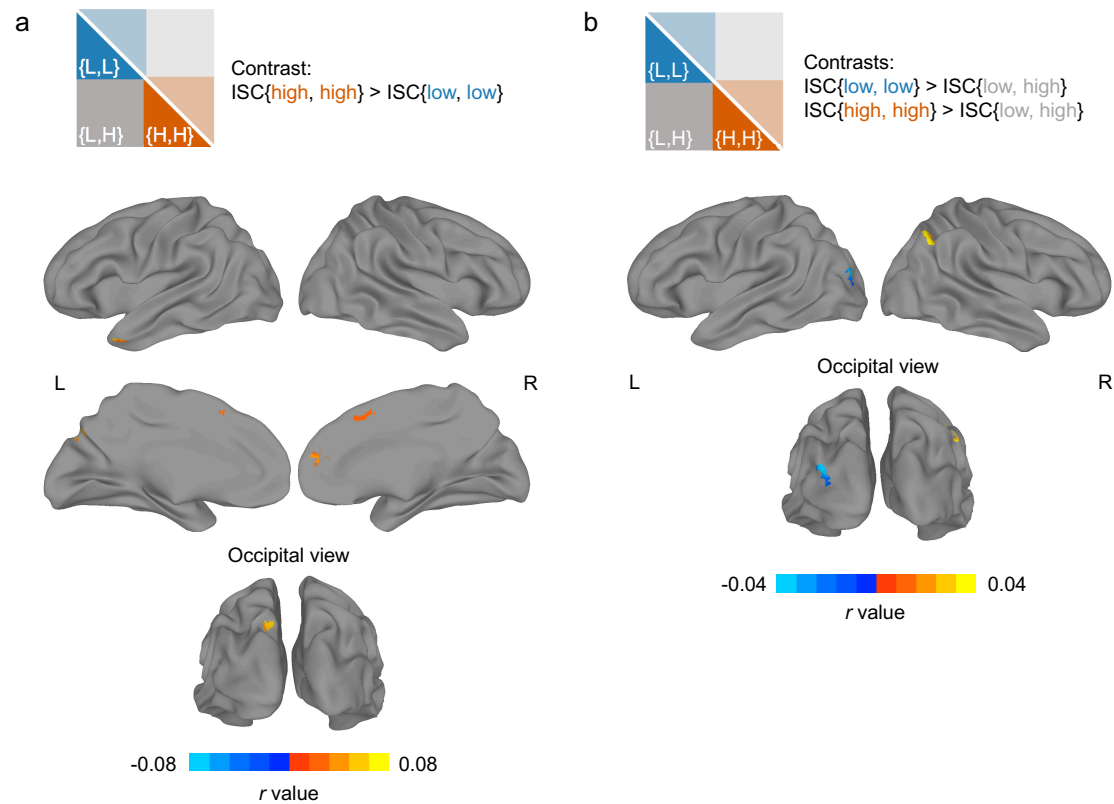
817  
818  
819  
820  
821  
822  
823  
824  
825  
826  
827  
828  
829  
830  
831  
832  
833  
834

**Figure 1. Experimental protocol, distribution of trait-level paranoia and inter-subject correlation analysis.** a) Schematic of experimental protocol. Participants came to the laboratory for an initial behavioral visit, during which they completed several computerized cognitive tasks as well as self-report psychological scales, one of which was the Green et al. Paranoid Thoughts Scale (GPTS)<sup>21</sup>. To minimize demand characteristics and/or priming effects, the fMRI scan visit took place approximately one week later. During this visit, subjects listened to an ambiguous social narrative in the scanner and then completed an extensive post-narrative battery consisting of both free-speech prompts and multiple-choice items. b) Distribution of scores on the GPTS-A subscale across  $n = 22$  participants, and median split used to stratify participants into low ( $\leq 18$ , blue) and high ( $\geq 19$ , orange) trait-level paranoia. c) Schematic of inter-subject correlation (ISC) analysis. Following normalization to a standard template, the inter-subject correlation of activation timecourse during narrative listening was computed for each voxel ( $v$ , yellow square; enlarged relative to true voxel size for visualization purposes) for each pair of subjects ( $i, j$ ), resulting in a matrix of pairwise correlation coefficients ( $r$  values). These values were then compared across paranoia groups using voxelwise linear mixed-effects models with crossed random effects to account for the non-independent structure of the correlation matrix<sup>22</sup>.



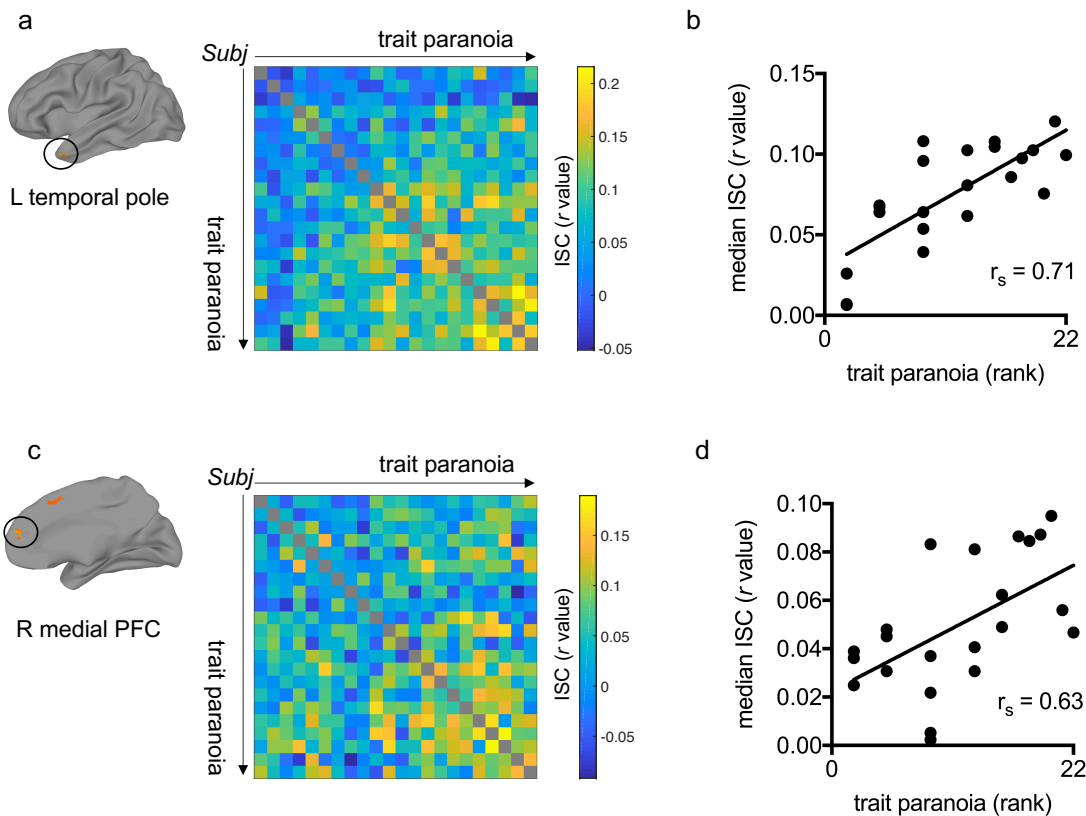
835  
836  
837  
838  
839  
840  
841  
842  
843  
844

**Figure 2. Narrative listening evokes widespread inter-subject correlation across the whole sample.** Voxels showing significant inter-subject correlation (ISC) across the timecourse of narrative listening in all participants ( $n = 22$ ). As expected, the highest ISC values were observed in auditory cortex, but several regions of association cortex in the temporal, parietal, frontal and cingulate lobes as well as the cerebellum also showed high synchrony. Also included are three representative axial slices from the cerebellum. Results are displayed at a voxelwise false-discovery rate (FDR) threshold of  $q < 0.001$ .



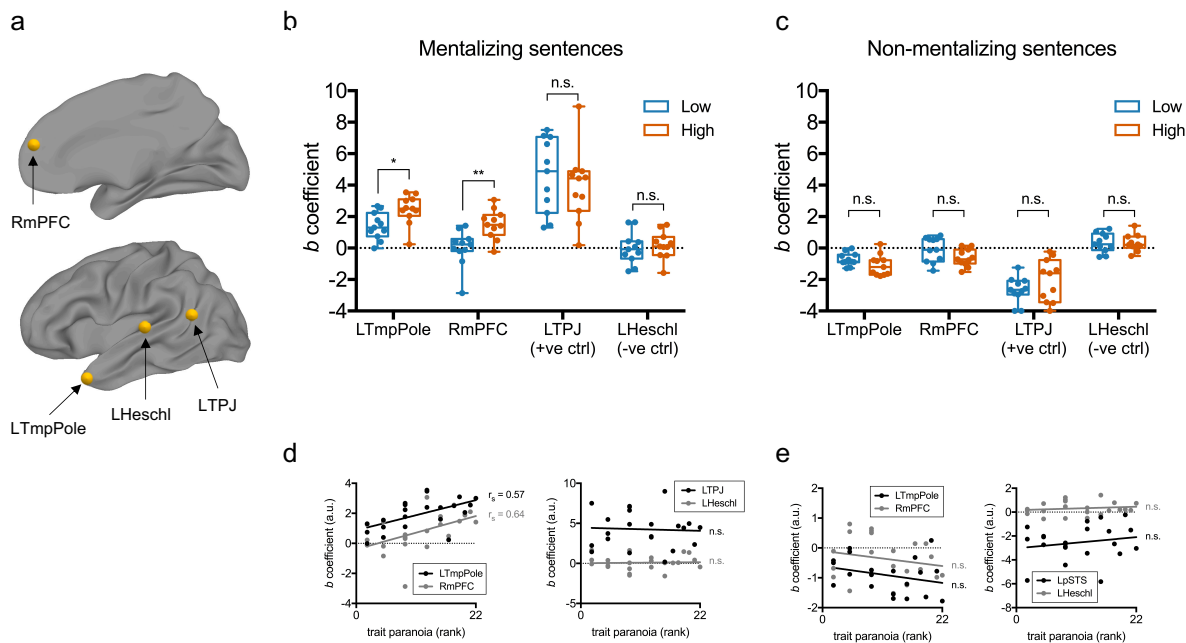
845  
846  
847  
848  
849  
850  
851  
852  
853  
854  
855  
856  
857  
858  
859  
860

**Figure 3. Trait-level paranoia modulates patterns of inter-subject correlation during narrative listening.** a) Results from whole-brain, voxelwise contrast revealing brain regions that are more synchronized between pairs of high-paranoia participants than pairs of low-paranoia participants (contrast schematized in top panel, cf. Fig. 1C). Significant clusters were detected in the left temporal pole, two regions in the right medial prefrontal cortex (one anterior and one dorsal and posterior), and the left precuneus. No clusters were detected in the opposite direction (low > high). b) Results from two whole-brain, voxelwise contrasts revealing brain regions that are more synchronized within a paranoia group than across paranoia groups. The first contrast revealed that left lateral occipital cortex was more synchronized within the low-paranoia group (i.e., low-low pairs) than across groups (i.e., high-low pairs; contrast schematized in top panel, cf. Fig. 1C). The second contrast revealed that right angular gyrus was more synchronized within the high-paranoia group (i.e., high-high pairs) than across groups. For all three contrasts, results are shown at an initial threshold of  $p < 0.002$  with cluster correction corresponding to  $p < 0.05$ .



861  
862  
863  
864  
865  
866  
867  
868  
869  
870  
871  
872  
873  
874  
875  
876  
877  
878  
879

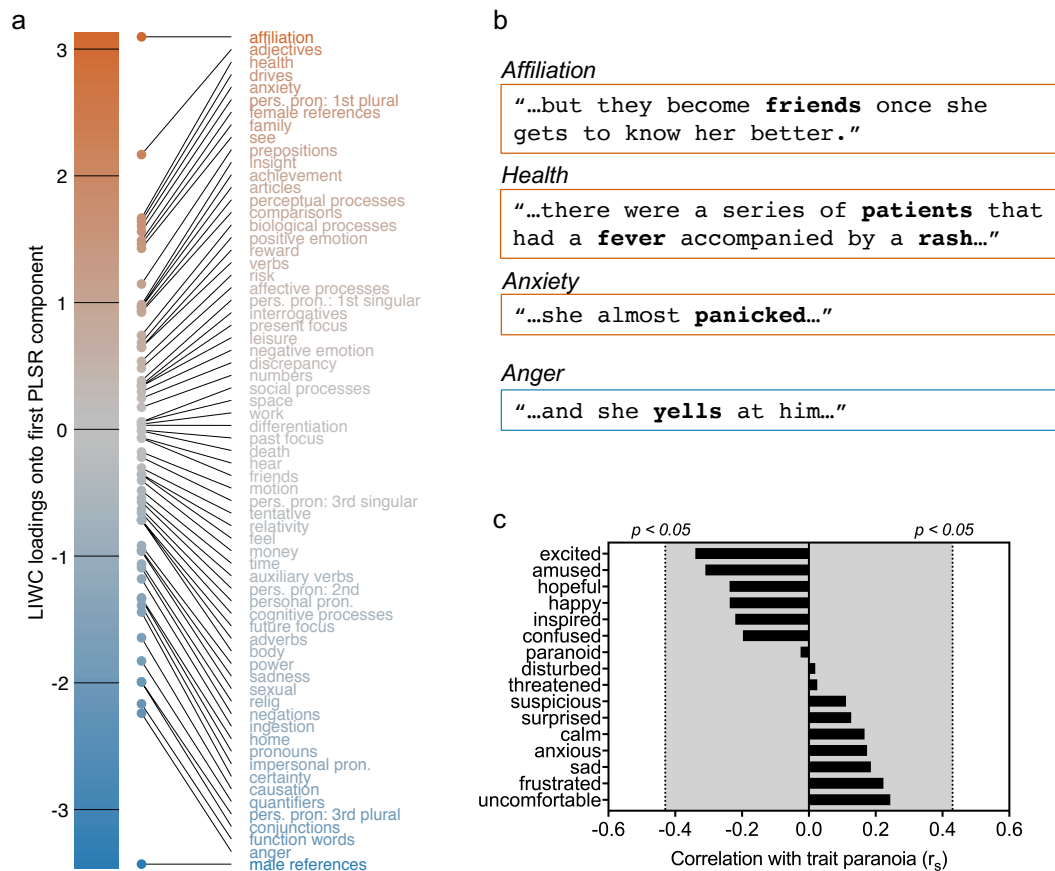
**Figure 4. Inter-subject correlation scales continuously with trait paranoia.** Post-hoc analyses for two regions of interest (ROIs) that emerged from the dichotomized contrast between high- and low-paranoia groups (cf. Fig. 3a): left temporal pole (top row) and right medial prefrontal cortex (PFC, bottom row). a) Location of ROI (left) and participant-by-participant inter-subject correlation (ISC) matrix (right) for the left temporal pole. Participants are ordered by increasing trait paranoia score. Each matrix element reflects the correlation between two participants' activation timecourses in the left temporal pole during narrative listening. Higher correlations are visible as one moves to the right and down along the diagonal, representing pairs of increasingly high-paranoia individuals. b) Scatter plot of paranoia rank versus median ISC value—i.e., the median of each row of the ISC matrix in (a). Each dot represents a participant. Rank correlation indicates a significant monotonic relationship between trait paranoia and median ISC in left temporal pole ( $r_s = 0.71$ ,  $p = 0.0002$ ). c) Location of ROI and participant-by-participant ISC matrix for the right medial PFC. Participants are ordered as in (a). d) Scatter plot of each participant's paranoia rank versus their median ISC value in the right medial PFC. As in (b), rank correlation indicates a significant monotonic relationship between paranoia rank and median ISC ( $r_s = 0.63$ ,  $p = 0.0016$ ).



880  
881

882 **Figure 5. Response to mentalizing events is stronger in high- compared to low-paranoia**  
 883 **individuals.** a) Regions of interest (ROIs) for the event-related analysis. LTmpPole, left temporal  
 884 pole; RmpFC, right medial prefrontal cortex; LTPJ, left temporo-parietal junction; LHeschl, left  
 885 Heschl's gyrus. b) Comparison of beta coefficients for each ROI for the mentalizing-events  
 886 regressor between paranoia groups (low, blue; high, orange). Each dot represents a subject. Boxes  
 887 represent the median and 25<sup>th</sup>/75<sup>th</sup> percentiles, and whiskers represent the minimum and maximum.  
 888 \* $p = 0.01$ ; \*\* $p < 0.007$ ; n.s., not significant (p-values adjusted to control the false discovery rate).  
 889 c) Comparison of beta coefficients for each ROI for the non-mentalizing-events regressor (the  
 890 inverse of the mentalizing-events regressor shown in (b)). Each dot represents a subject. Boxes  
 891 represent the median and 25<sup>th</sup>/75<sup>th</sup> percentiles, and whiskers represent the minimum and maximum.  
 892 d) Beta coefficients for the mentalizing-events regressor plotted against paranoia rank (coefficients  
 893 are the same as in (b)). Left panel: the two ROIs in which beta coefficient was hypothesized to  
 894 scale with trait paranoia (LTmpPole and RmpFC). Right panel: the two control ROIs (LTPJ and  
 895 LHeschl). Correlations between paranoia rank and beta coefficient: LTmpPole,  $r_s = 0.57$ ,  $p =$   
 896  $0.005$ ; RmpFC,  $r_s = 0.64$ ,  $p = 0.001$ ; LTPJ,  $r_s = -0.04$ ,  $p = 0.86$ , LHeschl,  $r_s = 0.02$ ,  $p = 0.95$ . e)  
 897 Beta coefficients for the non-mentalizing-events regressor plotted against paranoia rank  
 898 (coefficients are the same as in (c)). Left and right panels as in (d). Correlations between paranoia  
 899 rank and beta coefficients (all n.s.): LTmpPole,  $r_s = -0.28$ ,  $p = 0.21$ ; RmpFC,  $r_s = -0.22$ ,  $p = 0.33$ ;  
 900 LTPJ,  $r_s = 0.085$ ,  $p = 0.71$ ; LHeschl,  $r_s = 0.17$ ,  $p = 0.44$ .





901  
902  
903  
904  
905  
906  
907  
908  
909  
910  
911  
912  
913

**Figure 6. Speech analysis reveals a signature of trait-level paranoia in behavioral response to the narrative.** a) Loadings of all semantic and syntactic categories for the first component from a partial least squares regression relating features of speech during narrative recall to trait-level paranoia score, sorted by strength and direction of association with paranoia (those positively related to paranoia at top in orange; those inversely related at bottom in blue). b) Example sentences from participant speech transcripts containing words falling into the three of the top positive categories (affiliation, health and anxiety) and one of the top negative categories (anger). c) Rank correlations between participants' trait-level paranoia and their self-report measures of 16 emotions following the narrative (self-report was based on a Likert scale from 1 to 5). Dotted lines represent approximate threshold for a significant correlation a  $p < 0.05$  (uncorrected). Gray shaded area indicates non-significance.

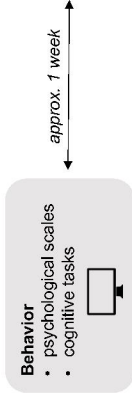
		Categorical (low vs. high)		Continuous	
		<i>t</i>	<i>p</i>	Spearman <i>r</i>	<i>p</i>
Demographics	Age	0.81	0.43	-0.11	0.62
	Sex*	1.64	0.20	--	--
	Education (yrs)	-0.24	0.81	-0.15	0.49
Cognitive ability	Working memory: Letter n-back (precision)	-0.45	0.66	0.16	0.47
	Fluid intelligence: Raven's matrices (total correct of 9 items)	0.00	1.00	-0.03	0.89
	Vocabulary: WRAT Word Reading (total correct of 42 items)	-1.42	0.17	0.31	0.16
	Verbal IQ: Penn logical reasoning test (total correct of 8 items)	0.23	0.82	-0.01	0.96
	Words of 6+ letters (free recall)	-1.03	0.32	0.04	0.85
	Words per sentence (free recall)	0.31	0.76	-0.18	0.43
fMRI data quality	Head motion (mean FD; mm)	0.94	0.36	0.01	0.96
	No. frames censored	-0.70	0.49	-0.08	0.74
	Average tSNR	-1.12	0.28	0.23	0.30
Attention to stimulus	No. comprehension questions correct	-0.31	0.76	0.08	0.72
	Total word count, free recall	1.00	0.33	-0.26	0.24
	Self-reported attention	0.48	0.63	-0.02	0.95
	Self-reported engagement	0.89	0.39	-0.10	0.65

914

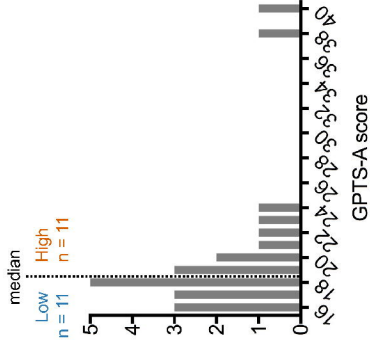
915 **Table 1. Trait paranoia was unrelated to potential confounding variables.** There were no  
916 significant differences between high- and low-paranoia participants in terms of demographics,  
917 cognitive abilities, fMRI data quality or attention to the stimulus. Categorical comparisons were  
918 carried out using Student's t-tests between the low and high paranoia groups as determined by  
919 median split (degrees of freedom for all t-tests = 20). Continuous comparisons were carried out  
920 using Spearman (rank) correlation between raw paranoia score and the variable of interest. All p-  
921 values are raw (uncorrected). \*Measured with a chi-squared test. FD, framewise displacement;  
922 tSNR, temporal signal-to-noise ratio; WRAT, Wide Range Achievement Test.

a

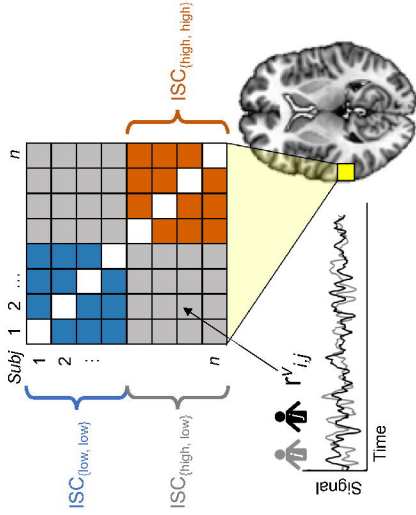
Visit 2

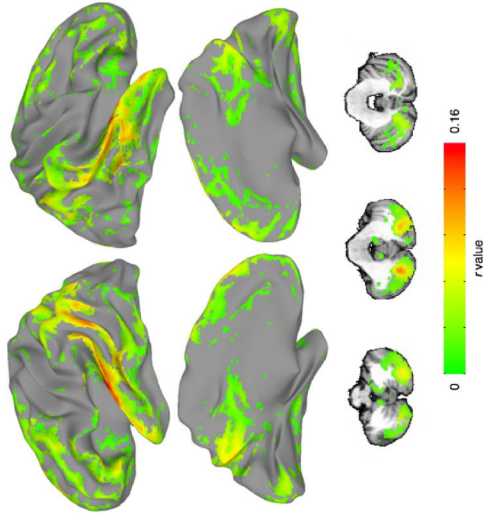


b



c

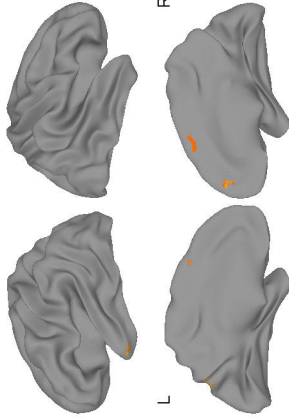




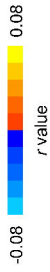
a



Contrast:  
 $ISC\{high, high\} > ISC\{low, low\}$



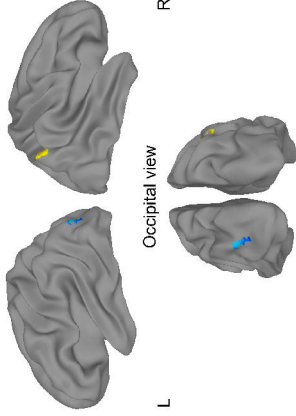
Occipital view



b

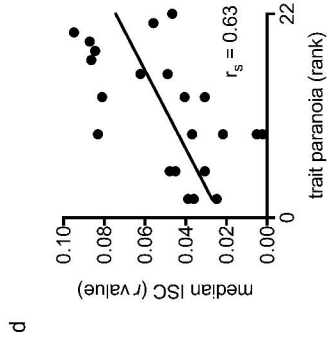
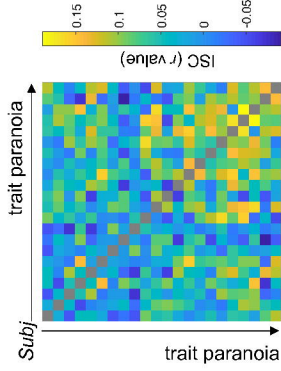
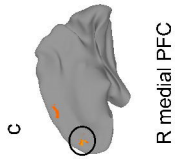
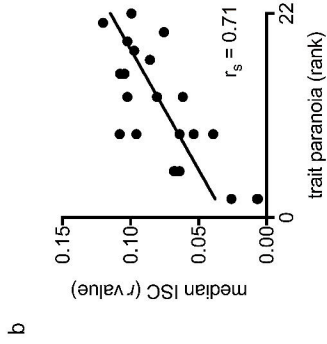
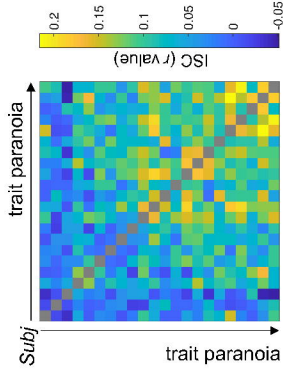
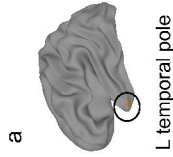


Contrasts:  
 $ISC\{low, low\} > ISC\{low, high\}$   
 $ISC\{high, high\} > ISC\{low, high\}$

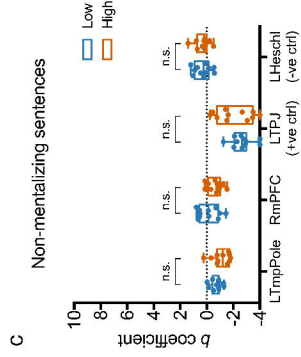
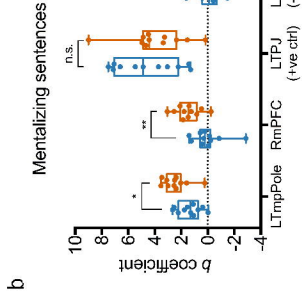
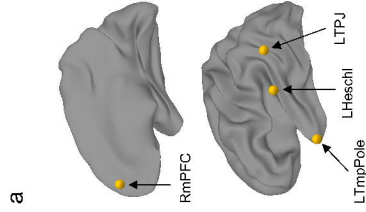


Occipital view

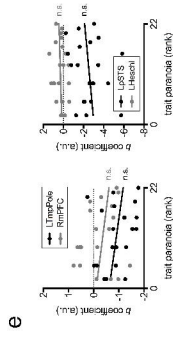
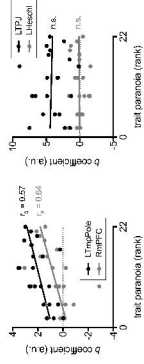


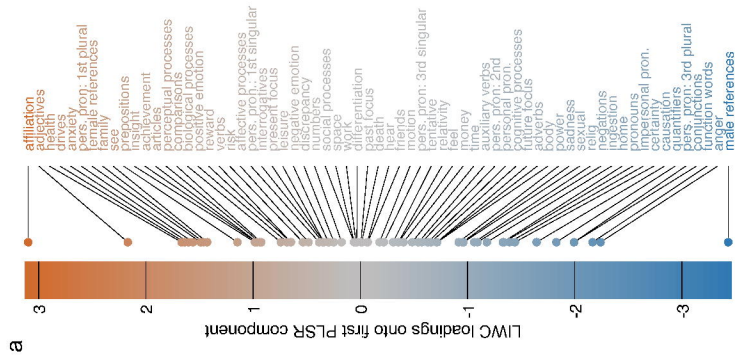






**d**





**b**

### Affiliation

"...but they become **friends** once she gets to know her better."

### Health

"...there were a series of **patients** that had a **fever** accompanied by a **rash**..."

### Anxiety

"...she almost **panicked**..."

### Anger

"...and she **yells** at him..."

**c**

